The Institution of Engineers, Australia

Determination of Wind Loads for an Arch Roof

J.D. HOLMES, M.I.E.Aust.

Determination of Wind Loads for an Arch Roof

J.D. HOLMES, M.I.E.Aust.*

SUMMARY A procedure used for determination of wind loads on a roof of a hangar, supported by a steel trussed arch with a quarter circle profile is described.

Fluctuating pressures from a boundary-layer wind tunnel model were used to determine the peak values of the support reactions, and of the bending moments and axial thrusts. Fifty-year return period responses were determined using meteorological data for the site. Comparisons are made of the results with the wind loads derived from Australian Standard AS 1170 Part 2.

1. INTRODUCTION

Wind loads, on low-rise buildings and other stiff structures for which resonant dynamic response can be neglected, are normally determined by direct application of codes and standards such as the Australian Standard AS 1170 Part 2[1]. However this Standard, in paragraph 2.1, also allows the use of wind tunnel tests and detailed meteorological data, including information on wind directions, for more accurate determination of wind loads.

Such a detailed study is described in this paper for a hangar with a circular arch roof at Woomera, SA, under renovation by the Department of Housing and Construction. Wind tunnel tests were carried out in the boundary-layer wind tunnel at James Cook University, Townsville, Queensland. In the tests, fluctuating pressures were measured on panels covering both a central and end bay of the roof. Data from these tests were used, subsequently, to calculate the expected maximum and minimum values, for a given wind speed and direction, of the support reactions, bending moments, and axial forces in the trussed arch members supporting these bays. Using wind speed and direction data for the site, predictions of long-term responses for each parameter were then made allowing for the variation of response with wind direction.

The study provided an additional source of data on pressure coefficients on curved roofs. The data in the Australian Standard have their origin in smooth flow tests carried out more than fifty years ago in the USSR[2].

2. WIND TUNNEL TESTS

2.1 Experimental Techniques

The wind tunnel at James Cook University has been described in detail elsewhere[3]. The test section is 2.5 m wide, 2.0 m high and 17.3 m long (extended in 1980). The tests for this study were carried out with the model mounted on the upwind turntable, allowing 12 m of upwind floor roughness to be used.

A rural atmospheric boundary layer, to match the geometric scaling ratio of 1/200 chosen for the model, was simulated. The floor roughness (carpet) was augmented by a 200 mm-high plain fence spanning the start of the test section floor.

Mean velocity and longitudinal turbulence intensity profiles were measured just upwind of the turntable. Good fits to logarithmic laws to a scaled height of about 100 m, with a full-scale roughness length* of 20 mm, were found. At the reference height of 10 m (50 mm in the wind tunnel), the turbulence intensity is about 17%. The longitudinal turbulence spectrum, showing the energy content of the turbulent velocity fluctuations as a function of frequency, was found to match well the standard von Karman-Harris spectrum[4,5] with a length scale appropriate to the roughness length of 20mm. This flow was thus a good simulation of that over smooth open country terrain representing that surrounding Woomera.

The building model was manufactured from 'Perspex' and wood. The circular arc roof was made from a section cut from perspex tube, to which emery paper was glued. The emery paper was an attempt to force the airflow over the roof into a fully rough, high Reynolds Number regime, more representative of full-scale conditions.

The full-scale dimensions of the building are shown in Figure 1. The exterior dimensions of the ventilator on the apex of the roof were modelled and attached to the model for most of the tests. However, for some tests this was omitted to determine its effect on pressures. The venting characteristics of the ventilator were not modelled, however, and no internal pressures were measured. The exterior pressures measured were thus representative of those on the full-scale structure with all openings sealed.

The main doors of the building were enclosed by a gantry housing at the sound end of the building

* Paper previously presented at the Metal Structures Conference, I.E. Aust., Brisbane, May 18-20 1983. (Paper C1509 submitted 4 April 1984)

* the roughness length z_o is a measure of the surface roughness and appears in the logarithmic law for mean wind up to about 100 m in the atmospheric boundary layer: u = a constant x $(\log_e z/z_o)$ where z is height above the surface.

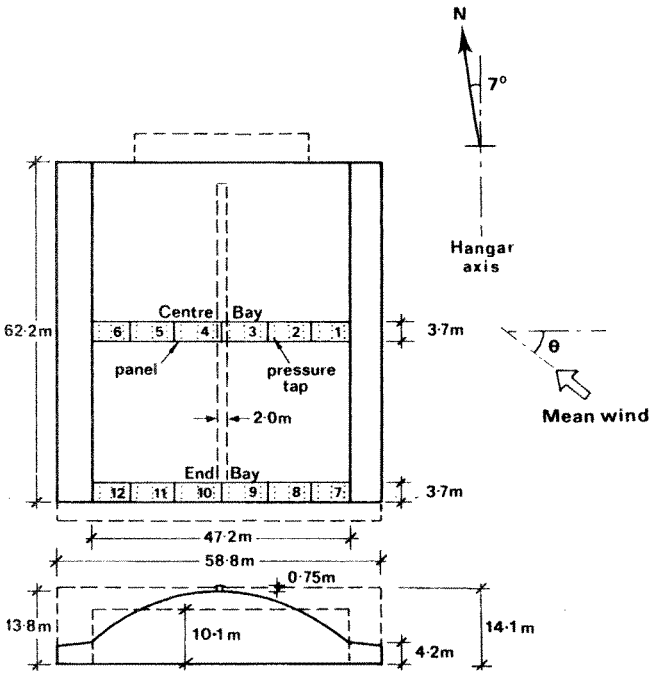

Figure 1 Dimensions of building (full-scale); pressure taps and panels

(Figure 1). The height of this enclosure was 14.1 m, i.e. slightly higher than the apex of the main arch profile of the main structure. This geometric feature could be expected to have a significant effect on the wind loads on the adjacent end bay of the building.

As well as the orientation of the building relative to true north, Figure 1 shows the mean wind direction, θ, as defined and used in this paper.

Fifty-four pressure tap holes were drilled into each roof bay under investigation, as shown in Figure 1. Pressure tappings consisting of pieces of steel tubing 10 mm long and 1 mm internal diameter, were glued into each hole. The pressure taps were connected by pieces of polythene tubing 50 mm long, to a 'Scanco' manifold connector, in groups of 9 - giving 6 panels per bay, as shown in Figure 1. The manifolds were connected by 450 mm lengths of polythene tubing, containing restrictors made from fine diameter hypodermic tubing, to 1 of 2 'Scanivalve' pressure scanning switches each containing a 'Setra' 237 pressure transducer. The frequency response of the tubing/manifold/restrictor/'Scanivalve' system had a 'half-power' point at about 100 Hz (equivalent to about 2 Hz in full-scale).

Using the switching capabilities of the 'Scanivalves', the panels were connected in pairs, covering all combinations within a bay, to the pressure transducers, which were sampled at 500 Hz for 16 second runs by a PDP 8/E minicomputer. On the latter mean, peak values, and coincident peak values were calculated.

2.2 Pressure Coefficient Definition

Pressures, forces, and structural effects on buildings, due to wind, fluctuate with time. The fluctuations include the longer periods associated with the passage of storms, and the micro-meteorological fluctuations of periods shorter than about 10 minutes, associated with the turbulence generated by the ground roughness. The latter fluctuations only are reproduced in the wind tunnel, but the longer-term fluctuations are inherent in the meteorological wind-speed data. To relate model measurements to full-scale building dimensions and wind speeds, the non-dimensional pressure coefficient is used, defined as follows:

$$C_p(t) = \frac{p(t) - p_o}{0.5\,\rho\,\bar{u}^2}$$

where p_o is the reference static (ambient) pressure and $\bar{u}$ is the reference mean velocity (10 minute mean).

In the present study, the reference velocity was measured at a height equivalent to 10 m upwind of the building. This height corresponds to the top of the gantry door on the hangar, and also to the airport anemometer position.

The three principal values of pressure coefficient are:

$$\text{Mean:}\quad \bar{C}_p(t) = \frac{\bar{p} - p_o}{0.5\,\rho\,\bar{u}^2}$$

$$\text{Maximum:}\quad \hat{C}_p(t) = \frac{\hat{p} - p_o}{0.5\,\rho\,\bar{u}^2}$$

$$\text{Minimum:}\quad \check{C}_p(t) = \frac{\check{p} - p_o}{0.5\,\rho\,\bar{u}^2}$$

where the symbols, -, $\hat{}$ and $\check{}$ denote mean, maximum, and minimum values respectively.

For the evaluation of structural internal forces and moments (Section 4), a series of coincident peak pressure coefficients were also required. These are defined in the following way:

$(C_{pj})_{\hat{i}}$ indicates the pressure coefficient on panel j when a maximum occurs on panel i,

$(C_{pj})_{\check{i}}$ is the pressure coefficient on panel j when a minimum value occurs on panel i.

The mean, maximum, and minimum pressure coefficients described in this paper were, in most cases, averages over 25 separate runs. The coincident peaks were averaged over 5 runs.

Pressure measurements were carried out for 45° increments of wind direction.

2.3 Measured Pressure Coefficients

The Appendix to this paper gives Tables of the mean, maximum, and minimum pressure coefficients for each of the wind directions tested, and for the 12 panels using the numbering system shown in Figure 1. Space limitations prohibit the inclusion of the coincident peak pressure coefficients, although these were an important part of the calculations of the structural loads (Section 4).

The mean pressure coefficients for the centre bay with the wind blowing normal to the apex (0°) are shown in Figure 2. For this wind direction, the ventilator has a considerable influence on the pressures on the centre bay. Without the vent, the flow accelerates over the centre part of the roof, giving high suctions on panels in this region. Intermittent reattachment occurs on the leeward side, giving relatively low suctions on the last

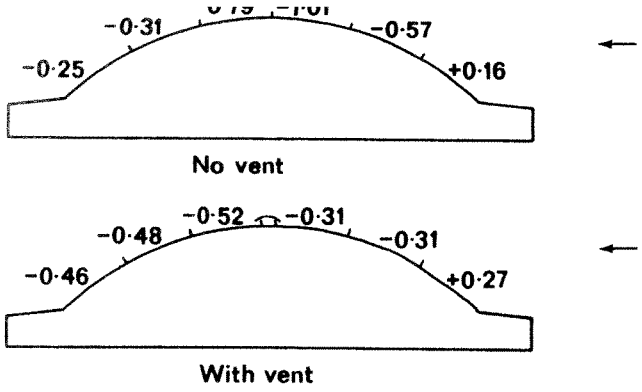

Figure 2 Mean pressure coefficients on centre bay ($\theta = 0^{o}$)

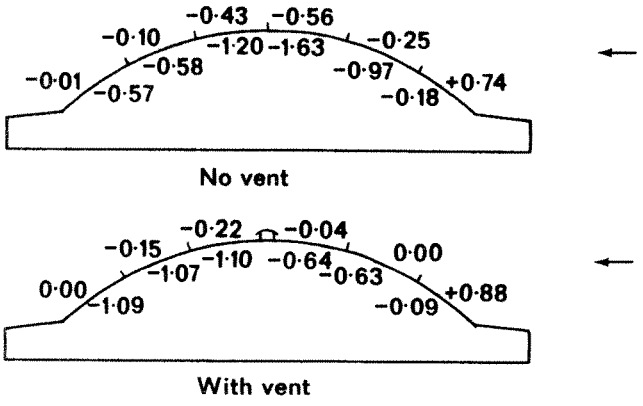

Figure 3 Peak pressure coefficients on centre bay ($\theta = 0°$) (maximum values shown above arch, minimum values below)

two panels. With the vent in position, some stagnation of the flow occurs in front of the vent, giving relatively low suctions on the second and third panels. Separation is initiated at the vent itself, and no significant reattachment occurs downwind, giving a larger wake region on the leeward side than occurs with no vent present.

Examples of peak (maximum and minimum) pressure coefficients are shown in Figure 3. These values are used together with the coincident peaks in estimating the structural loads (Section 4), but could also be used directly to design cladding for the panels. The effect of the vent is similar to the effect on the mean pressures, i.e., to reduce the suctions immediately upwind and downwind of the vent. However, the worst suctions on the two panels further downwind are increased.

3. STRUCTURAL ANALYSIS

Influence coefficients for support reactions, bending moments, and axial thrust were required. Figure 4 shows the dimensions and panel load positions assumed for the structural analysis. The profile of the actual trussed arch roof supports, approximates closely a quarter circle. For the analysis this profile was assumed, using the correct span of 45.72 m. This gives a rise of 9.47 m, compared with 9.33 m for the centreline of the actual trussed arch. The wind loads were assumed to act at the centroid of each panel, so unit loads for the calculation of influence coefficients were applied at the same positions. Unit loads were also

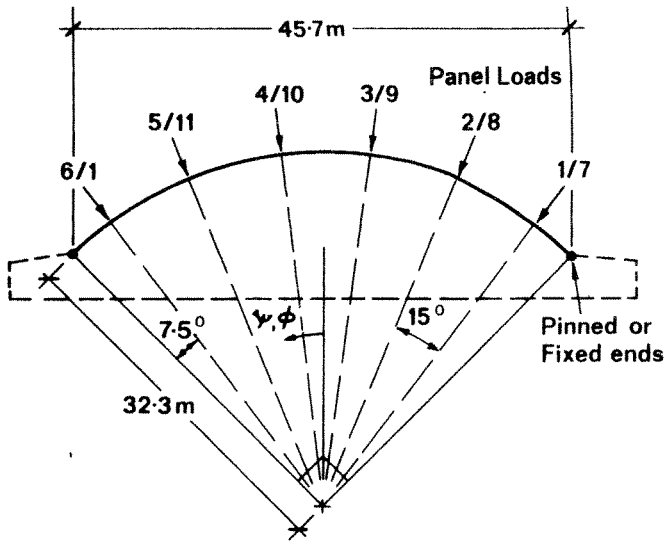

Figure 4 Dimensions and load positions for structural analysis

applied at intermediate positions to assist in the calculation of loads using AS 1170/2 pressure coefficients (see Section 6). Thus the unit loads were applied at 7.5° (Π/24 radians) angular increments along the span, denoted by ϕ in Figure 4. These angular positions were also the positions, denoted by ψ, at which bending moments and axial thrusts were determined.

Clearly, the linear elastic influence coefficients derived in this study are only valid for working stress design. However, analysis of the post-yield and plastic behaviour of steel structures under fluctuating wind loading is very complex [6, 7] and in its infancy.

Due to the uncertainty in the moment restraint at the supports of the arches in the prototype structure, calculations were carried out for both pinned supports (no moment restraint) and fixed supports (full moment restraint).

3.1 Pinned Arch

The two-pinned arch has one degree of statical indeterminancy. In a force method of analysis, the structure is reduced to a determinate primary structure and the unknown redundant force calculated from a superposition or compatibility equation. In this case, one of the pinned supports was reduced to a roller support, making the horizontal reaction, at that end, the unknown redundant. Applying a unit load at an arbitrary angular position, ϕ, the virtual work method was used to calculate the deflections (flexibility coefficients) required in the superposition equation. The superposition equation was then solved to give the unknown horizontal reaction. From this, expressions for the other support reactions, and bending moments and axial thrust along the arch were derived. Thus the influence coefficients for these parameters were derived.

3.2 Fixed Arch

The fixed or hingeless arch has three degrees of indeterminancy and, thus, three unknown redundants to be determined. A standard procedure is to reduce the structure to a curved cantilever by removing all restraint at one end, giving the two forces and one moment at that end as the redundants. The three

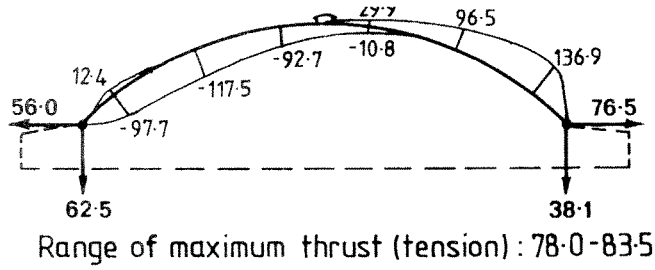

Figure 5 Expected peak values of bending moments, axial thrusts and reactions ÷ q (with vent; $\theta = 0^o$, centre bay)

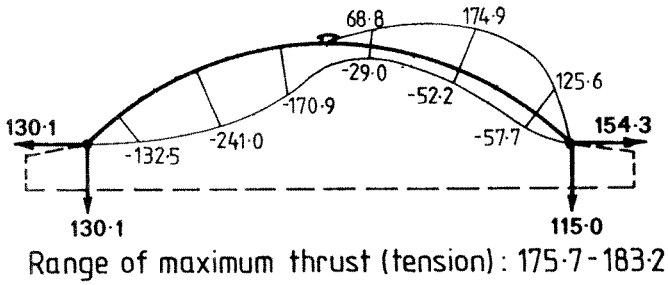

Figure 6 Expected peak values of bending moments, axial thrusts and reactions ÷ q (with vent; $\theta = 45^o$, end bay)

compatibility equations to be solved for these unknowns are known as the 'Arch Equations', and can be found in many structural analysis texts (e.g.[8]). The coefficients for these equations require the solution of several integrals. However, evaluation is straightforward with the quarter circle assumption. Once the redundant reactions have been determined, evaluation of the remaining reactions, bending moments, and axial thrusts, for an arbitrary unit load position, proceeds as for the pinned arch.

4. CALCULATION OF PEAK STRUCTURAL LOADS

The peak and coincident peak pressure coefficients described in Section 2.3 were used to estimate the limits of variation of various structural loads, for each bay, wind direction, and vent/no vent case. The method takes account of the partial correlation of the panel pressures with each other, and is described elsewhere[9]. Sample results for the pinned arch are shown in Figures 5 and 6. These values are the expected peak forces or moments divided by q, equal to 0.5 $\rho\bar{u}^2$. Thus the units for the forces are m^2, and for the moments, m^3. As the axial thrust varies little along the arch, only the range of values computed has been shown.

As expected, the bending moments on the fixed arch (not shown) are much lower than on the pinned arch, except near the supports. The reactions and axial thrusts are similar, however. For both support conditions, the end bay generally experiences higher values of all loads than the centre bay. The effect of the change of pressure distribution at 0^o wind direction, caused by the addition of the roof vent, is to reduce the reactions and axial thrusts. The bending moment distribution is also changed considerably, but the maximum values are increased by the addition of the vent. The highest bending moments occurred on the end bay for the 45^o wind direction (Figure 6). High reactions and axial thrust (tension) also occur for this case.

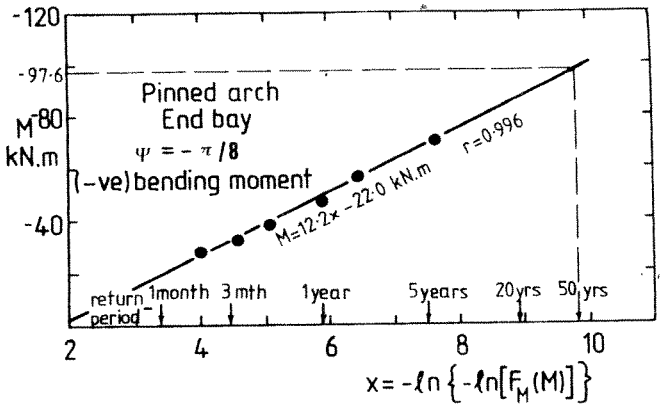

Figure 7 Extreme bending moment prediction (pinned arch, end bay)

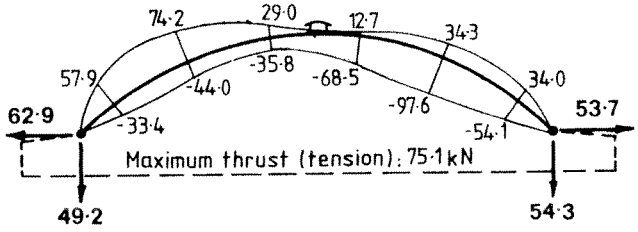

Figure 8 50-year return period predictions of responses (pinned arch; end bay, with vent. Forces in kN; moments in kN.m)

5. PREDICTION OF LONG-TERM EXTREME RESPONSES

Wind data were available for the Woomera site in the form of occurrences of the daily maximum gust above various speed levels. The direction of the wind gusts, i.e., one of 16 sectors, was also available.

The axis of the prototype hangar is orientated 7^o east of north (Figure 1). In order to use the wind data, pairs of adjacent wind directions were combined to approximate the directions for which the wind tunnel data were obtained. Thus, the north and north-north-east data were combined and used with the wind tunnel results for 0^o; the combined north-east and east-north-east data were used with the 45^o wind tunnel results, and so on.

The tabular data of wind speed, divided into 8 directions, were used with the response data in the following way. A table of daily maximum response was drawn up for each parameter so that daily exceedances of each response level for each direction were computed. The number of exceedances of the response level R, for any direction, was obtained from the number of exceedances of the wind speed, $u = \sqrt{(2R/\rho C_R)}$, where C_R is the (dimensional) coefficient, such as those shown in Figures 5 and 6.

The resulting daily exceedances for all directions were added together to give exceedances of each response level, independent of direction. Then a Fisher-Tippett Type I Extreme Value Distribution was fitted to the data for each response. A least-squares fit over a range of return periods from about two months to five years was carried out. An example of the fit for a bending moment is shown in Figure 7. In this figure r denotes correlation coefficient.

Examples of 50-year period predictions for the responses are shown in Figure 8. The predictions are, in many cases, dominated by the contribution from the 135° (south-westerly) direction.

As previously stated, the meteorological wind speed data are based on a daily maximum peak gust recorded at Woomera, by a Dines anemometer; this has been estimated to have an averaging period of 2 to 3 seconds. The wind tunnel data, on the other hand, were referenced to a mean wind speed of about 10 minutes' duration. Thus a conversion was required. Based on the work of Deacon[10], a value of $\hat{U}_{2sec.}/\overline{U}_{10\ min.})^2$ of 2.1 was used in the analysis described above.

6. COMPARISON WITH THE AUSTRALIAN STANDARD

The pressure coefficients derived from Figure C8 of AS 1170 Part 2[1] are shown in Figure 9. A wind direction of 0° is implied in the Standard. Two alternative values are specified for the windward quarter of the roof, as shown. The reference height for the pressure coefficients is not clearly stated in the Standard. A conservative interpretation would be to use the speed at the height of the highest point of the roof; the less conservative reference height of 10 m has been retained for the comparisons here.

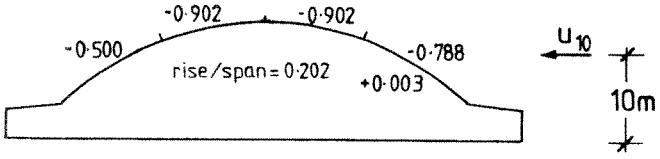

Figure 9 Pressure coefficients from AS 1170 Part 2 ($\theta = 0^o$)

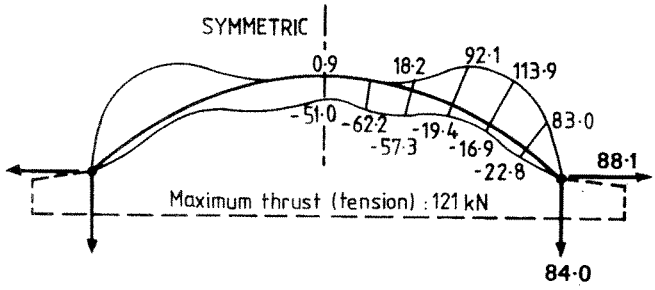

Figure 10 50-year return period predictions of response from AS 1170 Part 2 (pinned arch; end bay; moments in kN.m)

The pressure coefficients in Figure 9 can be compared with the measured mean pressure coefficients in Figure 2 and with the peak coefficients (divided by 2.1) in Figure 3. The Standard values are generally conservative, especially for the panels on top of the roof when the vent is added.

A reasonable interpretation of the Standard would use a pressure coefficient of -0.9 for the end bay of the building, for the 90° wind direction. This value is only slightly greater than the mean pressure coefficients recorded for the end bay for that wind direction (see Appendix). However, the value is exceeded by the measured values for the 45° wind direction. Clearly, the gantry housing plays an important part in determining the end bay pressures for these directions.

50-year return period values of the reactions, bending moments and axial thrusts can be derived from the Standard, for an end bay. The largest coefficients for the 0°, 90°, 180° and 270° directions have been combined with the design peak-gust wind speed of 43 m/s obtained from Table 2 of the Standard. The results of these calculations are shown in Figure 10. The values in Figure 10 do not include allowance for the new Area Reduction Factors for roofs, and the Wind Direction Factor, since these had not been incorporated into the Standard at the time the comparison was made.

The values in Figure 10 can be compared with those in Figure 8. The reactions, axial thrusts, and positive bending moments over most of the arch in the Standard substantially exceed the values derived from this study. However, the Standard underestimates the negative bending moments over a large part of the arch. This is partly because of the differences in pressure distributions, and hence bending moment distributions, for the 0° wind direction, mainly due to the effect of the vent. Another reason is the Standard's neglect of the 45° and 135° wind directions. The latter direction produced many of the largest loads in the present study. For these directions, the gantry housing would have had a significant effect on the loads on the end bay of the building, as noted previously.

7. CONCLUSIONS

Basic pressure coefficients, structural reactions, and axial forces and bending moments for a centre bay and an end bay of an arched hangar have been obtained from wind tunnel tests.

Wind speed and direction data for the site have been combined with the wind tunnel tests to produce predictions of long-term extreme responses. These may be used to assess the adequacy of the strength of the structure to resist future loads.

A comparison of the results with data derived from the Australian Standard AS 1170 Part 2 shows the present Standard, despite the complex fluctuating pressure patterns on roofs and the complex influence lines for the loads, is not grossly in error in this rather severe test of the quasi-steady format of the Standard.

The Standard does not deal with the changes in external pressure distribution due to the roof vent or gantry door housing, nor allow for oblique wind directions. The latter produced the largest loads on the end bay in the present study. Future amendments to the Standard could remedy these deficiencies.

In general, however, wind tunnel tests of the type described here are advisable for buildings with any unusual geometric features if realistic design loads are to be determined.

8. ACKNOWLEDGEMENTS

The author is grateful for the co-operation of the Department of Housing and Construction in the sponsorship of this study, and acknowledges the permission of the First Assistant Secretary, Engineering, to publish this paper. The author gratefully acknowledges the assistance of Professor W.H. Melbourne, Monash University, and Dr C.M.L. Dorman, Department of Housing and Construction, for their data on wind speed and direction. The author thanks Messrs. G. McNealy and R.J. Roy of James Cook University, for their assistance during the wind tunnel testing.

9. REFERENCES

1. Standards Association of Australia, 'SAA Loading Code, Part 1 - Wind Forces', AS 1170, Part 2, 1983.

2. Bounkin, K., and Tcheremoukhin, A., 'Wind Pressures on Roofs and Buildings', Transactions Central Aero and Hydrodynamical Institute, Moscow, No.35, 1928.

3. Holmes, J.D., 'Design and Performance of a Wind Tunnel for Modelling the Atmospheric Boundary Layer in Strong Winds', James Cook University, Wind Engineering Report

4. Von Karman, T. 'Progress in the Statistical Theory of Turbulence', Proc. Nat. Acad. Sci., USA, Vo. 34, 1948, p. 530-539.

5. Harris R.I., 'Measurements of Wind Structure at Heights up to 598 ft above Ground level', Symposium on Wind Effects, Loughborough University, April 1968.

6. Vickery, B.J., 'Wind Action on Simple Yielding Structures', A.S.C.E., J. Eng. Mech. Div., Vol. 96., No. EM2, 1970, p. 107-120.

7. Best, R.J., 'The Behaviour of a Simple Structure Under a Simulated Wind Load', James Cook University, Townsville, B.E. Thesis, 1976.

8. Gregory, M.S., 'Linear Framed Structures', Longmans, London, (1966), p. 288-291.

9. Holmes, J.D., 'A New Technique for the Determination of Structural Loads and Effects on Low-Rise Buildings', in 'Wind Tunnel Modeling for Civil Engineering Applications'. (Ed. T. Reinhold.) Cambridge University Press, New York, (1982), p. 344-356.

10. Deacon, E.L., 'Wind Gust Speed-Averaging Time Relationship', Australian Meteorological Magazine, No.51, 1965, p.11-14.

APPENDIX

Table I - Mean Panel Pressure Coefficients - No Vent

Wind direction, θ	Panel Number: 1	2	3	4	5	6	7	8	9	10	11	12
0°	+.16	-.57	-1.01	-.79	-.31	-.25	+.12	-.54	-.71	-.68	-.48	-.26
45°	+.07	-.40	-.74	-.82	-.64	-.28	-.48	-.65	-.89	-1.14	-1.22	-.85
90°	-.25	-.32	-.32	-.32	-.32	-.25	-.74	-.79	-.84	-.84	-.79	-.74

Table II - Mean Panel Pressure Coefficients - With Vent

Wind direction, θ	Panel Number: 1	2	3	4	5	6	7	8	9	10	11	12
0°	+.27	-.31	-.31	-.52	-.48	-.46	+.18	-.44	-.51	-.54	-.47	-.42
45°	+.08	-.34	-.53	-.99	-.67	-.30	-.47	-.61	-.83	-1.18	-1.08	-.80
90°	-.26	-.32	-.33	-.33	-.32	-.26	-.80	-.86	-.87	-.87	-.86	-.80
270°	-.06	-.07	-.08	-.08	-.07	-.06	+.34	+.16	.00	.00	+.16	+.34
315°	+.13	-.27	-.42	-.81	-.52	-.29	+.40	-.24	-.50	-.45	-.20	-.08

Table III - Maximum Peak Panel Pressure Coefficients - No Vent

Wind direction θ	Panel Number: 1	2	3	4	5	6	7	8	9	10	11	12
0°	+.74	-.25	-.56	-.43	-.10	-.01	+.60	-.17	-.33	-.30	-.09	+.01
45°	+.48	-.13	-.34	-.42	-.31	-.01	+.12	-.15	-.35	-.55	-.57	-.38
90°	+.43	+.31	+.20	+.20	+.31	+.43	-.32	-.30	-.30	-.30	-.30	-.32

Table IV - Maximum Peak Panel Pressure Coefficients - With Vent

Wind direction, θ	Panel Number:											
	1	2	3	4	5	6	7	8	9	10	11	12
0^{o}	+.88	.00	-.04	-.22	-.15	.00	+.67	-.06	-.18	-.15	-.07	-.01
45^{o}	-.54	-.03	-.22	-.48	-.30	-.01	+.10	-.13	-.29	-.59	-.45	-.36
90^{o}	+.44	+.31	-.19	+.19	+.31	+.44	-.37	-.33	-.31	-.31	-.33	-.37
270^{o}	+.27	+.29	+.23	+.23	+.29	+.27	+1.20	+.91	+.40	+.40	+.91	+1.20
315^{o}	-.54	-.02	-.16	-.38	-.20	+.04	+1.22	+.33	-.11	-.08	+.23	+.36

Table V - Minimum Peak Pressure Coefficients - No Vent

Wind direction, θ	Panel Number:											
	1	2	3	4	5	6	7	8	9	10	11	12
0^{o}	-.18	-.97	-1.63	-1.20	-.58	-.57	-.21	-1.08	-1.27	-1.26	-1.18	-.66
45^{o}	-.19	-.82	-1.41	-1.45	-1.11	-.82	-1.50	-1.47	-1.64	-2.00	-2.30	-1.88
90^{o}	-.87	-1.01	-1.00	-1.00	-1.01	-.87	-1.59	-1.75	-1.88	-1.88	-1.75	-1.59

Table VI - Minimum Peak Pressure Coefficients - With Vent

Wind direction θ	Panel Number											
	1	2	3	4	5	6	7	8	9	10	11	12
0^{o}	-.09	-.63	-.64	-1.10	-1.07	-1.09	-.14	-.95	-1.04	-1.21	-1.16	-.98
45^{o}	-.21	-.71	-.93	-1.76	-1.13	-.85	-1.46	-1.39	-1.50	-2.13	-2.24	-1.67
90^{o}	-.82	-1.00	-.95	-.95	-1.00	-.82	-1.61	-1.82	-1.94	-1.94	-1.82	-1.61
270^{o}	-.44	-.49	-.42	-.42	-.49	-.44	-.16	-.40	-.38	-.38	-.40	-.16
315^{o}	-.15	-.65	-.81	-1.50	-1.01	-.77	-.04	-.77	-1.16	-1.16	-.74	-.53

J.D. HOLMES

John Holmes is a Principal Research Scientist at CSIRO Division of Building Research, Highett, Victoria. Although his original training was in aeronautical engineering, he has been involved in research and consulting on wind loading and other wind effects on structures since 1969. He has been actively involved in wind tunnel testing of major structures such as the West Gate Bridge, Melbourne, and City Corp building, New York. In recent years his interests have mainly been wind loads on low-rise buildings with extensive studies at James Cook University and CSIRO. He is a member of Committee BD/6/2 on Wind Loads of the Standards Association. He holds the degrees of B.Sc.(Eng.) (Southhampton) and Ph.D. (Monash).

CORRESPONDENCE ON THIS PAPER WILL BE ACCEPTED
FOR PUBLICATION UNTIL 28 FEBRUARY 1985